Improved Control Scheme for Low Voltage Ride-Through of PMSG-based Wind Energy Conversion Systems

Tan Luong Van, *Member, IEEE*, Trung Hieu Truong, Minh Tien Cao,
Phu Cong Nguyen and Hung Nguyen

Abstract-*This paper proposes a low-voltage ride-through (LVRT) scheme for the permanent magnet synchronous generator (PMSG) wind turbine system under grid voltage sags by exchanging of the control roles of the two converters and using the braking chopper (BC). The DC-link voltage is controlled at the machine-side converter (MSC) by applying the sliding mode control instead of the grid-side converter (GSC). The GSC regulates the grid active power for a maximum power point tracking (MPPT). The validity of this control algorithm has been verified by the simulation of the 2[MW]-PMSG wind turbine system.*

Keywords: ***Braking chopper, permanent magnet synchronous generator, ride-through, wind turbine.***

I. INTRODUCTION

In the recent years, the wind power generation has been concerned as one of the most rapidly growing energy sources in the world since the natural resources are becoming exhausted. Compared with the doubly fed induction generator (DFIG) wind systems, a direct-drive wind energy conversion system based on permanent magnet synchronous generator (PMSG) has a lot of advantages such as no gearbox, high precision, high power density, and simple control method, except initial installation costs [1], [2].

A demanding requirement for wind farms is the fault ride-through capability. According to this demand, the wind turbine is required to survive during grid voltage faults. The ability of a wind turbine to survive for a short duration of voltage dip without tripping is often referred to as the low voltage ride-through (LVRT) capability of a turbine. An LVRT techniques required for wind turbine systems is shown in Fig. 1 [3].

Several solutions have been proposed for the low voltage ride-through (LVRT) techniques in the variable-speed wind turbine systems. For this purpose, a braking chopper (BC) including an external resistor is connected in the rotor-side of the doubly-fed induction generator to absorb the active power during the grid fault [4], [5]. However, it is not so easy to improve the power quality at the output of the wind turbine systems since the BC can just dissipate the power. In other way, the STATCOM has been applied to keep the wind turbine system connected to the grid during grid faults [6]. With this method, the voltage regulation is much improved in both the transient state and the steady-state. Nevertheless, the STATCOM must be used together with the BC circuit which protects the RSC from the rotor overcurrent when the grid fault happens.

In the PMSG wind turbine system, the STATCOM has been employed to keep the wind turbine system connected to the grid during the grid faults [7], [8]. By using this method, the regulation of the voltage is significantly improved. However, the STATCOM cannot be used alone without the BC. Another different solution which employs the energy storage system (ESS) can offer a ride-through capability and suppress the output power fluctuations of the wind turbine systems [9], [10]. In this method, to reduce the power capacity of the ESS which can absorb the full differential power during the grid fault, the generator speed can be increased to store the kinetic energy in the system inertia. However, the cost of the ESS system designed in the case of the deep voltage is too expensive.

Normally, DC-link voltage is controlled to be a constant at the grid-side converter, while the machine-side converter controls the active power for the maximum power point tracking (MPPT). In the case of the grid voltage sags, the GSC in the conventional control method may be out of control. When the grid fault occurs, the DC-link voltage is excessively increased since the wind turbine (WT) continues its operation to generate power to the grid. However, the overall generated output power cannot deliver to the grid fully.

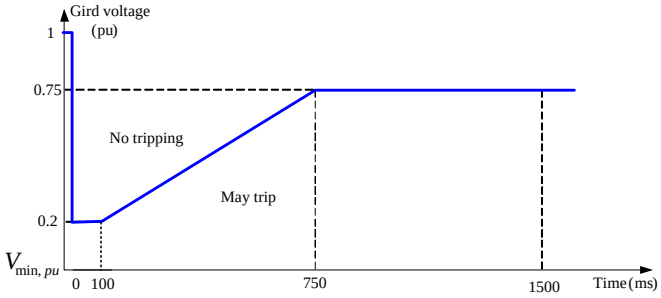


Fig. 1. *A gried code [3].*

A few research results have been suggested that employ the DC-link voltage control strategies by the machine-side converter instead of the GSC [11], [12]. By

Research was supported by Ho Chi Minh City University of Food Industry.

T. L. Van and P. C. Nguyen are with the Department of Electrical and Electronic Technology, Ho Chi Minh city University of Food Industry, Ho Chi Minh 700000, Vietnam (Tel: +84-909653157, e-mail: luonghepc@gmail.com, congnp@cntp.edu.vn).

T. H. Truong and H. Nguyen are with HUTECH Institute of Engineering, HUTECH University of Technology, Ho Chi Minh 700000, Vietnam (e-mail: hieuhepc@gmail.com, n.hung@hutech.edu.vn).

M. T. Cao is with Faculty of Telecommunications Engineering, Telecommunications University, Nha Trang 650000, Vietnam (e-mail: caominhtienkvtd@gmail.com).

this, the DC-link voltage can be controlled to be constant by increasing the generator speed during the grid voltage sag. However, the DC-link voltage response is not good although a hybrid adaptive proportional–integral (PI) controller based on the power and energy relationship is used [11].

In this paper, the DC-link voltage is controlled at the MSC by applying the sliding mode control. In the meanwhile, the power of the PMSG is controlled by the GSC. The GSC dual current controllers in the positive and negative-sequence reference frames are employed for grid unbalanced conditions. The validity of the control algorithm has been verified by simulation results for the PMSG wind power system.

II. Machine-side Converter Control

A. Nonlinear Modeling

To design the DC-link voltage controller, the dynamic characteristics of wind turbines in the PMSG wind power system are considered. Neglecting the loss of the converter, the generator power and the DC-link capacitor power can be expressed as

$$P_g = P_t - J_t\omega_t \frac{d\omega_t}{dt} - B_t\omega_t^2 - P_{g.loss} \quad (1)$$

$$P_{cap} = CV_{dc}\frac{dV_{dc}}{dt} = P_g - P_{grid} \quad (2)$$

where P_g is the generator power, P_{grid} is the grid power, $P_{g.loss}$ is the generator loss, P_{cap} is the DC-link capacitor power, V_{dc} is the DC-link voltage, C is the DC-link capacitor.

From Eq. (1) and Eq. (2), a dynamic equation for the PMSG wind turbine system is expressed as

$$P_{grid} = P_t - J_t\omega_t \frac{d\omega_t}{dt} - B_t\omega_t^2 - P_{g.loss} - CV_{dc}\frac{dV_{dc}}{dt} \quad (3)$$

A nonlinear relation between V_{dc} and ω_t is shown in Eq. (3).

B. DC-link Voltage Control

A single-input and single-output nonlinear system is expressed as [13], [14]

$$\dot{x} = f(x) + g(x)u \quad (4)$$

$$y = h(x) \quad (5)$$

where x is the state vector, u is the control input, y is the output, f and g are the smooth vector fields, respectively, and h is the smooth scalar function.

The nonlinear equations in Eq. (1) and Eq. (2) are expressed in the form of Eq. (4) as follows:

$$\begin{bmatrix}\dot{V}_{dc}\\ \dot{\omega}_t\end{bmatrix} = \begin{bmatrix}-\frac{P_{grid}}{CV_{dc}}\\ \frac{P_t}{J_t\omega_t} - \frac{B_t\omega_t}{J_t} - \frac{P_{g.loss}}{J_t\omega_t}\end{bmatrix} + \begin{bmatrix}\frac{1}{CV_{dc}}\\ -\frac{1}{J\omega_m}\end{bmatrix}\cdot P_g \quad (6)$$

In Eq. (6), the DC-link voltage V_{dc} is selected as an output. A relation between input and output should be delivered. So, the output y in Eq. (5) is differentiated as [14]

$$\dot{y} = \nabla h(f + g\cdot u) = L_f h(x) + L_g h(x)\cdot u \quad (7)$$

where $L_f h(x)$ and $L_g h(x)$ represent Lie derivatives of $h(x)$ with respect to $f(x)$ and $g(x)$, respectively. The Lie derivative is defined as [14]

$$L_f h = \nabla h f = \frac{\partial h}{\partial x}\cdot f \quad (8)$$

If $L_f h$ and $L_g h$ are replaced to *A(x)* and *E(x)*, the output of the system is obtained as

$$\dot{y} = A(x) + E(x)u \quad (9)$$

where

$$A(x) = -\frac{1}{CV_{dc}}P_{grid} \text{ and } E(x) = \frac{1}{CV_{dc}}$$

If a control input *u* is chosen as

$$u = E^{-1}(x)[-A(x) + v] \quad (10)$$

where *v* is the equivalent control input to be specified.

The sliding surface (*s*) is defined as

$$s = e + k_1\int e\,dt + k_2\iint e\,dt \quad (11)$$

where $e = y - y^*$, y^* is the tracking reference, and k_1, and k_2 are the positive constant gains.

By using a sliding mode control (SM) theory, the equivalent control input can be derived as

$$u = E^{-1}(x)\left[-A(x) + \dot{e} - k_1 e - k_2\int e\,dt\right] + \gamma sgn(s) \quad (12)$$

where γ>0.

The requirements for an existence condition of the sliding mode can be proved by Lyapunov theory [14] as

$$\begin{aligned} W &= s\cdot s' \\ &= s\left[-A(x) + \dot{e} - k_1 e - k_2\int e\,dt\right] \\ &= -g(x)\gamma\|s\|_1 \le 0 \end{aligned} \quad (13)$$

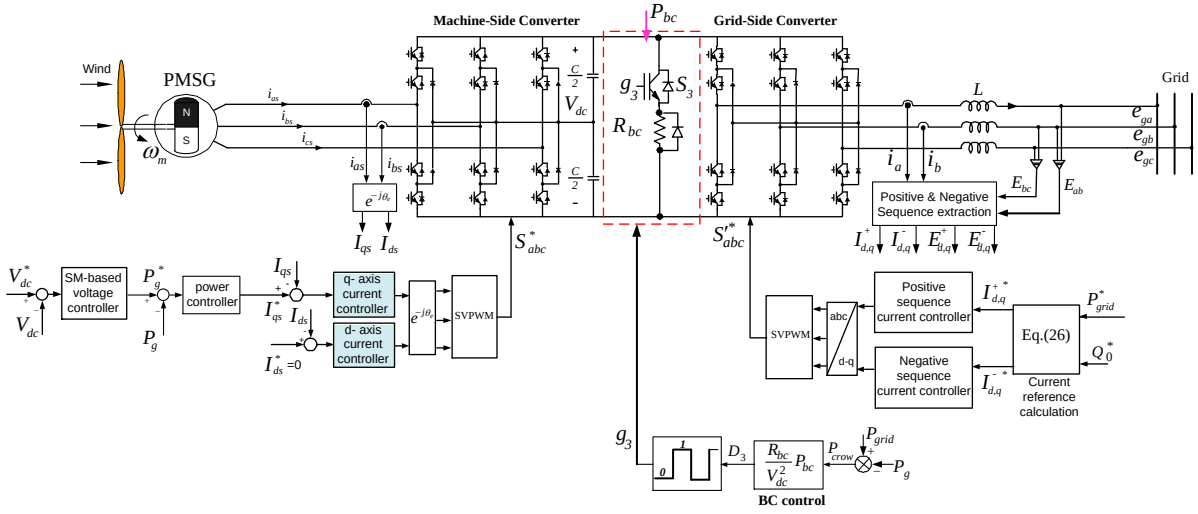


Fig. 2. *Control block diagram of overall system.*

The operation of the GSC is directly affected by the unbalanced grid voltage, in which the generator power delivered to the grid is restricted. During this grid fault duration, the wind turbine and generator should keep operating as if they do in the normal condition. Thus, the power transferred from the generator side may make an increase in the DC-link voltage. Differently from the conventional control of the AC/DC converter, the DC-link voltage is controlled by the machine-side converter instead of the GSC. The basic principle is that the generator-side converter should try to adjust the generator output power to balance the load power need, such that the DC-link voltage can be maintained (Fig. 2).

III. GRID-SIDE CONVERTER CONTROL

In unbalanced grid voltage conditions, the positive-sequence voltage component in the stationery reference frame is expressed as [15]

$$\begin{bmatrix} e_{ga}^{+} \\ e_{gb}^{+} \\ e_{gc}^{+} \end{bmatrix} = \begin{bmatrix} \frac{1}{6}(2e_{ga}-e_{gb}-e_{gc}) - \frac{1}{j2\sqrt{3}}(e_{ga}-e_{gc}) \\ \frac{1}{6}(2e_{gb}-e_{gc}-e_{ga}) - \frac{1}{j2\sqrt{3}}(e_{gc}-e_{ga}) \\ \frac{1}{6}(2e_{gc}-e_{ga}-e_{gb}) - \frac{1}{j2\sqrt{3}}(e_{ga}-e_{gb}) \end{bmatrix} \quad (14)$$

where e_{ga}, e_{gb}, e_{gc} and e_{ga}^{+}, e_{gb}^{+}, e_{gc}^{+} are the instantaneous grid voltages and the positive-sequence components, respectively. The *j* in Eq. (14) means the phase shift of 90 degrees, which is obtained by using all-pass filters [15]. The d-axis voltage calculated from the positive-sequence component of the grid voltages is controlled to be zero, from which the reference phase angle for control is determined.

The apparent power delivered to the grid under unbalanced conditions is expressed in terms of the positive and negative sequence components as [16]

$$S = 1.5\left(e^{j\omega t}e_{dqs}^{+} + e^{-j\omega t}e_{dqs}^{-}\right)\left(e^{j\omega t}i_{dqs}^{+} + e^{-j\omega t}i_{dqs}^{-}\right)^{*} \quad (15)$$

where the superscript of "*" represents a complex conjugate value, and the superscripts "+" and "-" are the positive- and negative-sequence components, respectively.

Thus, the apparent power is divided into the active power *p(t)* and the reactive power *q(t)* [16]

$$p(t) = P_0 + P_{c2}\cos(2\omega t) + P_{s2}\sin(2\omega t) \quad (16)$$

$$q(t) = Q_0 + Q_{c2}\cos(2\omega t) + Q_{s2}\sin(2\omega t) \quad (17)$$

where

$$P_0 = 1.5(E_d^{+}I_d^{+} + E_q^{+}I_q^{+} + E_d^{-}I_d^{-} + E_q^{-}I_q^{-})$$
$$P_{c2} = 1.5(E_d^{+}I_d^{-} + E_q^{+}I_q^{-} + E_d^{-}I_d^{+} + E_q^{-}I_q^{+})$$
$$P_{s2} = 1.5(E_d^{+}I_q^{-} - E_q^{+}I_d^{-} - E_d^{-}I_q^{+} + E_q^{-}I_d^{+})$$
$$Q_0 = 1.5(-E_d^{+}I_q^{+} + E_q^{+}I_d^{+} - E_d^{-}I_q^{-} + E_q^{-}I_d^{-})$$
$$Q_{c2} = 1.5(-E_d^{+}I_q^{-} + E_q^{+}I_d^{-} - E_d^{-}I_q^{+} + E_q^{-}I_d^{+})$$
$$Q_{s2} = 1.5(E_d^{+}I_d^{-} + E_q^{+}I_q^{-} - E_d^{-}I_d^{+} - E_q^{-}I_q^{+})$$

From Eq. (16) and Eq. (17), the power (P_0, Q_0, P_{s2}, P_{c2}) can be represented in a matrix form as

$$\begin{bmatrix} P_0 \\ Q_0 \\ P_{s2} \\ P_{c2} \end{bmatrix} = 1.5\begin{bmatrix} E_d^{+} & E_q^{+} & E_d^{-} & E_q^{-} \\ E_q^{+} & -E_d^{+} & E_q^{-} & -E_d^{-} \\ E_q^{-} & -E_d^{-} & -E_q^{+} & E_d^{+} \\ E_d^{-} & E_q^{-} & E_d^{+} & E_q^{+} \end{bmatrix}\begin{bmatrix} I_d^{+} \\ I_q^{+} \\ I_d^{-} \\ I_q^{-} \end{bmatrix} \quad (18)$$

The second-order components of power (P_{c2}, P_{s2}) due to the unbalanced grid voltage fluctuates not only the DC-

link capacitor power but also the real power delivered to the grid. These two components are controlled to zero to eliminate the power fluctuations. The real power reference (P^*_{grid}) is obtained from (1), in which P_t is calculated from the MPPT method [13]. The reactive power reference (Q^*_0) can be determined from unity power factor operation or the grid requirements. Thus, the positive- and negative-sequence components of the current references are expressed as

$$\begin{bmatrix} I_d^{+*} \\ I_q^{+*} \\ I_d^{-*} \\ I_q^{-*} \end{bmatrix} = \frac{2}{3} \begin{bmatrix} E_d^+ & E_q^+ & E_d^- & E_q^- \\ E_q^+ & -E_d^+ & E_q^- & -E_d^- \\ E_q^- & -E_d^- & -E_q^+ & E_d^+ \\ E_d^- & E_q^- & E_d^+ & E_q^+ \end{bmatrix}^{-1} \begin{bmatrix} P^*_{grid} \\ Q^*_0 \\ 0 \\ 0 \end{bmatrix} \quad (19)$$

The control block diagram of the GSC that includes the current controller for positive- and negative-sequence components is shown in Fig. 2.

IV. Braking Chopper Control

The braking chopper will be activated to dissipate the rest of the power, P_{bc} as

$$P_{bc} = P_g - P_{grid} \quad (20)$$

As shown in Fig. 2, the braking chopper is controlled by the switch S_3. The duty ratio D_3 for the switch depends on P_{bc}, which is expressed as

$$D_3 = \frac{R_{bc}}{V_{dc}^2} P_{bc} \quad (21)$$

where R_{bc} is the braking resistance.

V. Simulation Results

To verify the effectiveness of the proposed method, the simulation has been carried out using the PSIM software for a 2-MW PMSG wind turbine. The parameters of the wind turbine and generator are listed in Table 1 and 2, respectively. The DC-link voltage is controlled at 1,300[V], the DC-link capacitance is 0.1[F], the switching frequency is 2[kHz], and the grid voltage is 690[V_{rms}]/60[Hz].

TABLE 1. PARAMETERS OF WIND TURBINE

Rated power	2 [MW]
Blade radius	45 [m]
Air density	1.225[kg/m^3]
Max. power conv. coefficient	0.411
Cut-in speed	3[m/s]
Cut-out speed	25[m/s]
Rated wind speed	16.1 [m/s]
Blade inertia	6.3x10^6[kg.m^2]

TABLE 2. PARAMETERS OF 2[MW] PMSG

Rated power	2 [MW]
Grid voltage	690 [V]
Stator voltage/frequency	690[V]/60[Hz]
Stator resistance	0.008556[Ω]
d-axis inductance	0.00359[H]
q-axis inductance	0.00359[H]

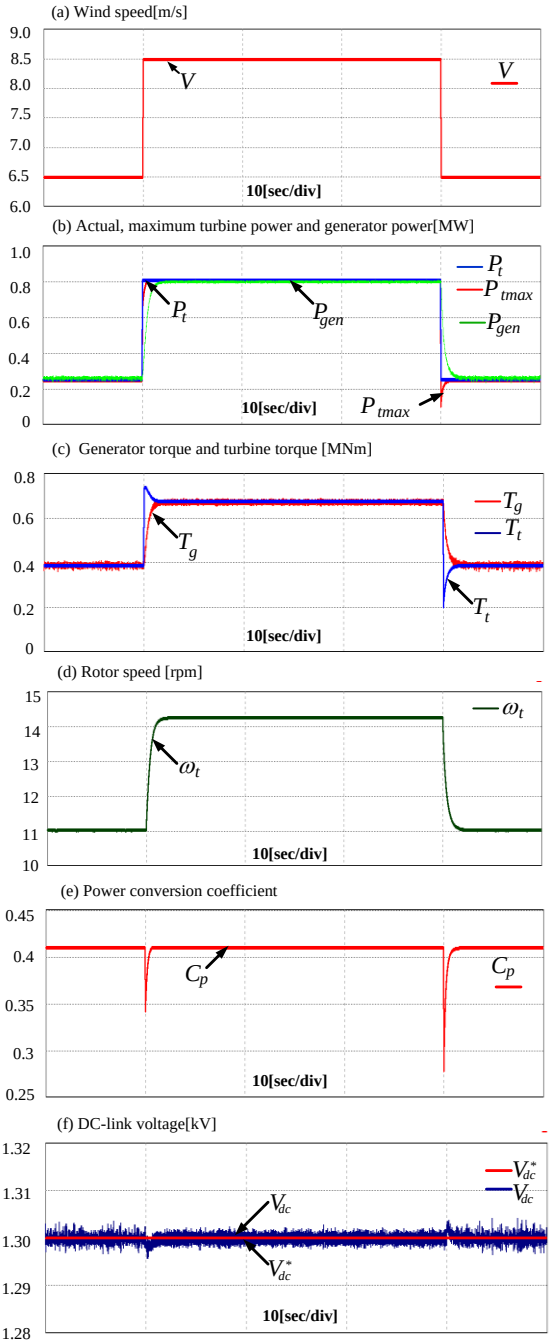


Fig. 3. *Responses of optimal power control in step-wise wind speed variation under normal grid voltage. (a) Wind speed. (b) Actual and maximum available turbine power and generator power. (c) Generator and Turbine torque. (d) Power conversion coefficient. (e) Rotor speed. (f) DC-link voltage.*

Fig. 3 shows the system performance under the normal grid condition. The wind speed is shown in Fig. 3(a). The turbine and generator power, turbine and generator torque, rotor speed and power conversion coefficient are shown from Fig. 3(b) to (e), respectively. In this case, the generator is controlled to keep the DC-link voltage constant, of which variation is less than 1[%] as shown in Fig. 3(f).

Fig. 4 shows the system performance for a grid unbalanced voltage sag, in which the wind speed is assumed to be constant (8[m/s]) for easy examination. The fault condition is 30% sag for three phases, for 1 sec (60 cycles), which is between the point ⓐ to ⓑ as shown in Fig. 4(a). Fig. 4(b) shows the magnified grid voltages and the magnified grid positive d-axis, respectively, for 6 cycles just before and after fault. Also, the reference phase angle for control is illustrated in Fig. 4(d). The grid currents in positive and negative sequence dq-axis are illustrated in Fig. 4(e) and 4(f). Due to the grid unbalanced voltage sag, the positive-sequence q-axis voltage is reduced and the negative-sequence d-q voltage components appear. During the grid fault duration, the generator speed is increased to keep the DC-link voltage constant as shown in Fig. 4(g). Also, the grid, generator and turbine powers are illustrated in Fig. 4(h). Fig. 4(i) shows the DC-link voltage response.

Fig. 5 shows the BC responses under balanced sags. Since the differntial power is not able to deliver to the grid, the rest of the power is dissipated by the BC. The switching pulse and the BC current are shown in Fig. 5(a) and (b), respectively.

Fig. 6 shows the DC-link voltage responses by using the conventional PI controller and the proposed method. The proposed method gives faster transient response and lower overshoot.

VI. CONCLUSION

The paper proposes a coordinated control scheme of grid-side converter, machine-side converter, and braking chopper for the LVRT in the permanent magnet synchronous generator wind turbine system. At the grid fault, a method is based on the DC-link voltage control at the machine-side converter using sliding mode control, while the MPPT strategy is applied to control the grid power at the grid-side converter. Also, BC is proposed to give an LRT capability for the wind turbines even though the grid voltage is much dropped. The validity of the control algorithm has been verified by simulation results for 2MW PMSG wind power system.

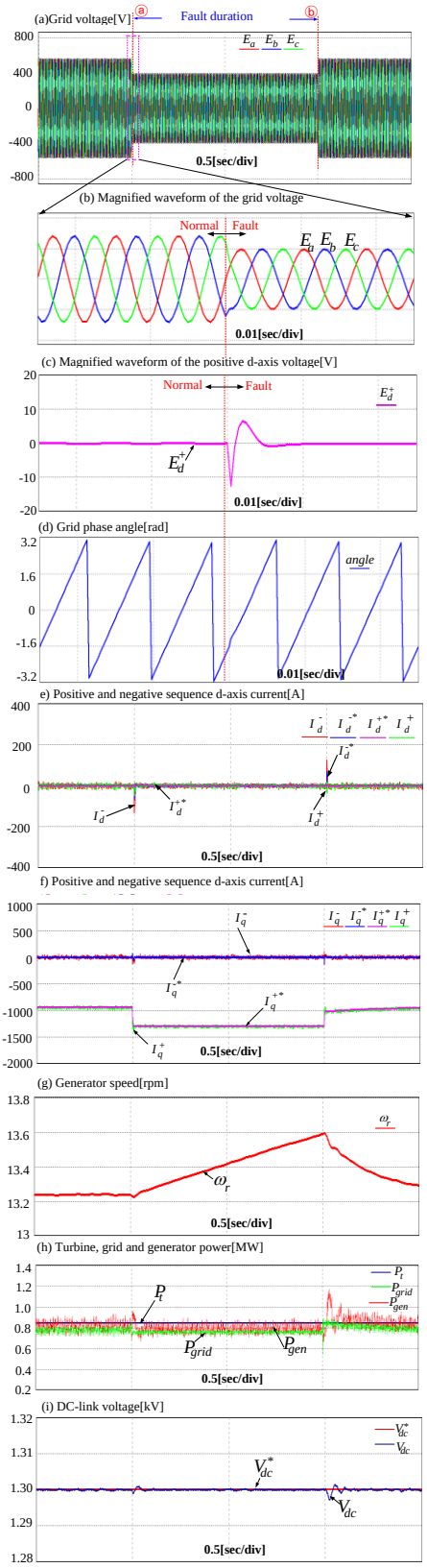


Fig. 4. *Wind generation performance for three-phase balanced voltage drops (30%). (a) Grid voltage. (b) Magnified waveform of the grid voltage. (c) Magnified waveform of positive d-axis voltage. (d) Angle. (e) Positive and negative sequence d-axis grid currents. (f) Positive and negative sequence q-axis grid currents. (g) Generator speed. (h) Turbine, grid and generator power. (i) DC-link voltage.*

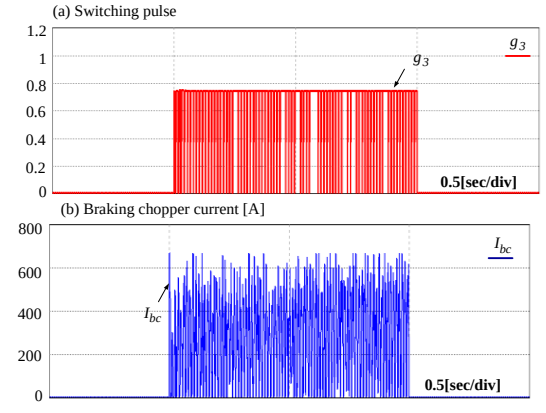


Fig. 5. *Performance of BC under balanced sags. (a) Switching pulse. (b) Braking chopper current.*

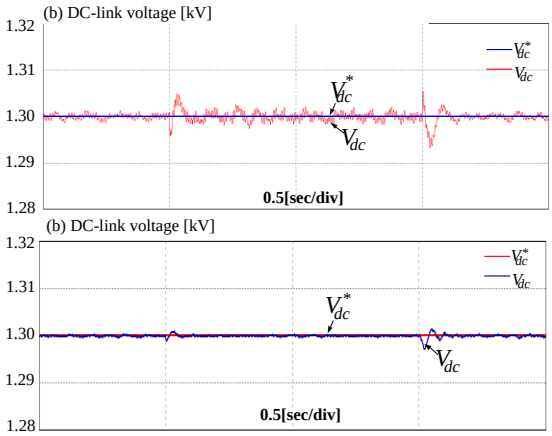


Fig. 6. *Performance of DC-link voltage control using: (a) conventional PI controller. (b) proposed method.*

ACKNOWLEDGMENT

This research was supported by Ho Chi Minh City University of Food Industry research grants.

REFERENCES

[1] M. Chinchilla, S. Arnaltes, and J. C. Burgos, "Control of permanent-magnet generators applied to variable-speed wind-energy systems connected to the grid," *IEEE Trans. Energy Convers.*, vol. 21, no. 1, pp. 130-135, Mar. 2006.

[2] H. Polinder, F. F. A van der Pijl, and P. Tavner, "Comparison of direct-drive and geared generator concepts for wind turbines," *IEEE Trans. Energy Convers.*, vol. 21, no.3, pp. 543-550, Sep. 2006.

[3] T. Ackermann, J. R. Abbad, I. M. Dudurych, I. Erlich, H. Holttinen, J. R. Kristoffersen, and P. E. Sorensen, "European balancing act," *IEEE Power and Energy Magazine*, Vol. 5, No. 6, pp. 90–103, Nov./Dec. 2007.

[4] F. K. A. Lima, A. Luna, P. Rodriguez, E. H. Watanabe, and F. Blaabjerg, "Rotor voltage dynamics in the doubly fed induction generator during grid faults," *IEEE Trans. Power Electron.*, vol. 25, no. 1, pp. 118–130, Jan.2010.

[5] L. G. Meegahapola, T. Littler, and D. Flynn, "Decoupled-DFIG fault ridethrough strategy for enhanced stability performance during grid faults," *IEEE Trans. Sustainable Energy*, no. 3, pp. 152–162, Oct. 2010.

[6] W. Qiao, G. K. Venayagamoorthy, and R. G. Harley, "Real-time implementation of a STATCOM on a wind farm equipped with doubly-fed induction generator," *IEEE Trans. Ind. App.*, Vol. 45, No.1, pp. 98-107, Jan./Feb. 2009.

[7] B. Singh, R. Saha, A. Chandra, and K. Al-Haddad, "Static synchronous compensators (STATCOM): A review," *IET Power Electron.*, vol. 2, no. 4, pp. 297–324, 2009.

[8] T. H. Nguyen, D.-C. Lee, T. L. Van, and J.-H. Kang, "Coordinated Control of Reactive Power between STATCOM and Wind Farms for PCC Voltage Regulation", *Journal of Power Electronics*, Vol. 13, No. 5, pp. 909-918, Sep. 2013.

[9] T. H. Nguyen, and D.-C. Lee, "Ride-through technique for PMSG wind turbines using energy storage systems,"*Journal of Power Electronics*, vol. 10, iss. 6, pp. 297–324, 2010.

[10] M. R. Abedi and K. Y. Lee, "Smart energy storage system for integration of PMSG-based wind power plant," *2015 IEEE Power & Energy Society General Meeting*, 2015, pp.1-5.

[11] X. Yuan, F. Wang, D. Boroyevich, Y. Li, and R. Burgos, "DC-link voltage control of a full power converter for wind generator operating in weak-grid systems," *IEEE Trans. Power Electron.*, vol. 24, no. 9, pp. 2178–2192, Sep. 2009.

[12] M. Davari and Y. A.-R. I. Mohamed, "Robust DC-Link Voltage Control of a Full-Scale PMSG Wind Turbine for Effective Integration in DC Grids," *IEEE Trans. Power Electron.*, vol. 32, no. 5, pp.4021–4035, May, 2017.

[13] T. L. Van, N. M. D. Nguyen, L. T. Toi and T. T. Trang, "Advanced Control Strategy of Dynamic Voltage Restorers for Distribution System Using Sliding Mode Control Input-Ouput Feedback Linearization", *Lecture notes in electrical engineering*, Vol. 465, pp.521-531, Dec., 2017.

[14] J. J. E. Slotine and W. Li, *Applied Nonlinear Control*. Englewood Cliffs, NJ: Prentice-Hall, 1991, pp. 207–271.

[15] G.-M. Lee, D.-C. Lee, and J.-K. Seok, "Control of series active power filters compensating for source voltage unbalance and current harmonics," *IEEE Trans. Ind. Applicat.*, vol. 51, no. 1, pp. 132-139, Feb. 2004.

[16] H.-S. Song and K. Nam, "Dual current control scheme for PWM converter under unbalanced input voltage conditions," *IEEE Trans. Ind. Applicat.*, vol. 46, no. 5, pp. 953-959, Oct. 1999.